Available online at www.eccomasproceedia.org
Eccomas Proceedia COMPDYN (2021) 4558-4567

ECCOMAS
Proceedia

COMPDYN 2021
8th ECCOMAS Thematic Conference on
Computational Methods in Structural Dynamics and Earthquake Engineering
M. Papadrakakis, M. Fragiadakis (eds.)
Streamed from Athens, Greece, 28 - 30 June 2021

NUMERICAL MODELING OF SLIP RESPONSE OF LATERALLY SWAYING BRIDGE PIERS' TENSILE REINFORCEMENT

Konstantinos G. Megalooikonomou[1]
[1] GFZ German Research Centre for Geosciences, Helmholtz Centre Potsdam, Helmholtzstraße 7, 14467 Potsdam, Brandenburg, Germany
e-mail: kmegal@gfz-potsdam.de

Abstract

Yield penetration occurs from the critical section towards both the shear span and the support of reinforced concrete columns; physically it refers to the extent of the nonlinear region and determines the pullout slip measured at the critical section. Contrary to the fixed design values adopted by codes of assessment, the yield penetration length is actually the only consistent definition of the notion of the plastic hinge length, whereas the latter determines the contribution of pullout rotation to column drift and column stiffness. Yield penetration in the anchored reinforcing bar inside the shear span of the column where it occurs, destroys interfacial bond between bar and concrete and reduces the strain development capacity of the reinforcement. This affects the plastic rotation of the member by increasing the contribution of bar slippage. Results obtained from the analytical procedures introduced in this paper are compared with experimental evidence from tests conducted on circular reinforced concrete bridge piers under cyclic loading designed and detailed according with Eurocode 8-II (2005). It can be seen that the produced monotonic envelope for applied shear load versus the slip of the extreme tensile reinforcing bar of the circular section of the bridge piers under study is in good agreement with the experimental results.

Keywords: yield penetration, bar slippage, circular bridge piers, pull-out rotation

ISSN:2623-3347
Peer-review under responsibility of the organizing committee of COMPDYN 2021.
doi: 10.7712/120121.8807.18441

1 INTRODUCTION

This paper presents a unidirectional bond model and its correlation with an experimental campaign of reinforced concrete bridge piers under cyclic excitation. The prototypes that were used in this study in order to determine the details of the specimens of the experimental study were monolithic concrete bridges located along the Egnatia highway [1] in Greece. The specimens (A1-A6) were designed to represent single column-to-superstructure connections. Four connection specimens (A1-A4) modeled at 1/5 scale the geometry and actions occurring in connections swaying in the direction perpendicular to the bridge axis (Fig. 1.a,b) whereas the remaining two specimens (A5,A6) modeled connections swaying in the direction parallel to the bridge axis (Fig.1c). In the remainder of this presentation these are denoted as group A specimens (A1-A6). All connections comprised a T-joint, but joint geometry and reinforcement arrangement were parameters of investigation (Fig. 2). Specimen A1 was designed and detailed according with EN 1998-2, 2005 [2] (Fig. 2). Specimen A2 was designed with the same geometry as A1, but with part of the required joint reinforcement placed in the primary beams adjacent to the joint. This alternative placement of joint shear reinforcement is allowed in EN 1998-2, 2005 [2] and CALTRANS (2004) [3] so as to avoid reinforcement congestion (Fig.2). Specimen A3 was designed with the same dimensions as A1, but with an inspection opening in the joint body in order to evaluate this construction practice in bridge monolithic joint connections (Fig. 2). Specimen A4 was designed with reduced cap beam width, in order to check whether the increased width for cap beams required by EN 1998-2, 2005 [2] is indeed an essential requirement (Fig.2). Specimen A5 was designed also according with EN 1998-2, 2005 [2], but it was tested for force and moment transfer acting in the direction of the bridge axis. This is the first reported beam-to-column specimen designed with a hollow section of beam (Fig. 2). Moreover, it has an opening for inspector passage in the joint panel (as in the case of specimen A3), in order to evaluate the influence of the openings when force transfer occurs in the longitudinal bridge axis (Fig. 2). Specimen A6 was designed with the same dimensions as A5, but without the opening for inspector passage in the joint panel.

All steel reinforcements used for the construction of the specimens were EN 1992, 2005 [4] compliant C500 deformed bars, with a nominal yield strength of f_y=500MPa, ratio of maximum strength to yield strength between 1.15 and 1.35 ($1.15 \leq f_u/f_y \leq 1.35$) and tension strain ductility at failure in excess of 7.5 ($\varepsilon_u/\varepsilon_y \geq 7.5$). Concrete material properties were determined from standard compression tests of 150x300 mm concrete cylinders that had been cast and cured along with the test specimens (Table 1, average values at time of component testing).

Table 1: Concrete material properties for all specimens [1].

Specimen		Days of test	f_{cm} (MPa)	$E_{cm,o}$ (MPa)
A1		176	27.55	9910
A2		251	29.14	12445
A3		259	29.30	11725
A4		302	29.85	10705
A5	beam	30	26.00	9440
	column	28	33.95	15595
A6	beam	88	26.30	5970
	column	86	45.00	14645

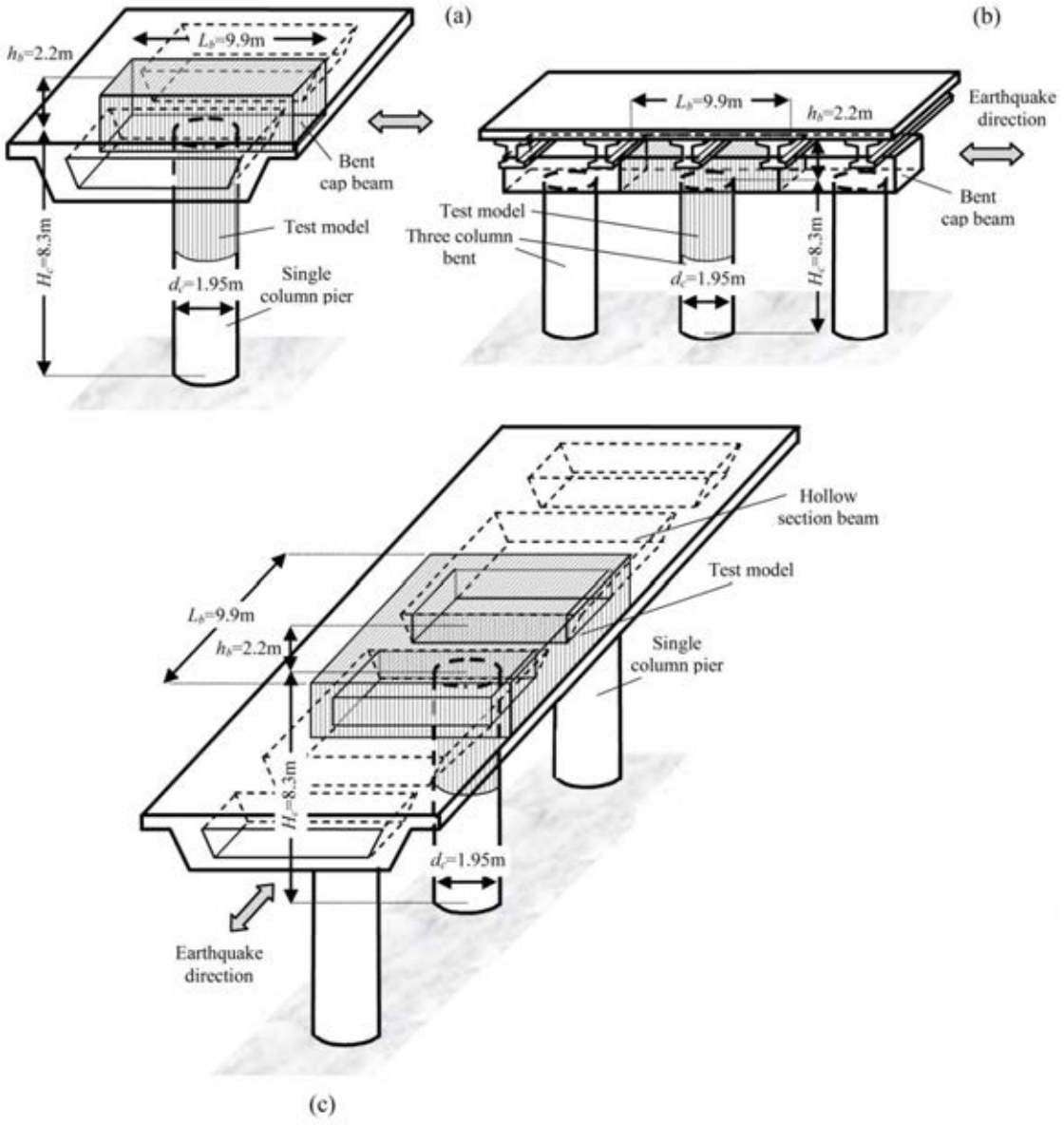

Figure 1: Representation of the prototype bridge structure commonly encountered in Egnatia Avenue and the test model for: (a-b) A1 to A4 specimens and (c) A5 and A6 specimens [1].

2 PROPOSED ALGORITHM OF THE UNIDIRECTIONAL BOND MODEL

The deformation capacity of frame elements comprises contributions of flexural, shear and reinforcement pullout components. The estimation of the available deformation capacity of a column is linked to the length of plastic hinges. Following an implicit assumption that all terms are additive, the flexural component of lateral displacement is obtained from the sum of an elastic component, owing to the flexural deformation occurring along the length of the member, and a plastic component that is practically owing to the inelastic rotation that occurs in the small region near the face of the support where moments may exceed the yielding limit. When comparing these deformation estimates with the experimental evidence from predominantly flexural components, it is found that there is a great disparity between measured and estimated deformation capacities characterized by notable scatter [5], [6]. Several attempts to identify the source of inaccuracy have motivated the progress made in that field, not the least

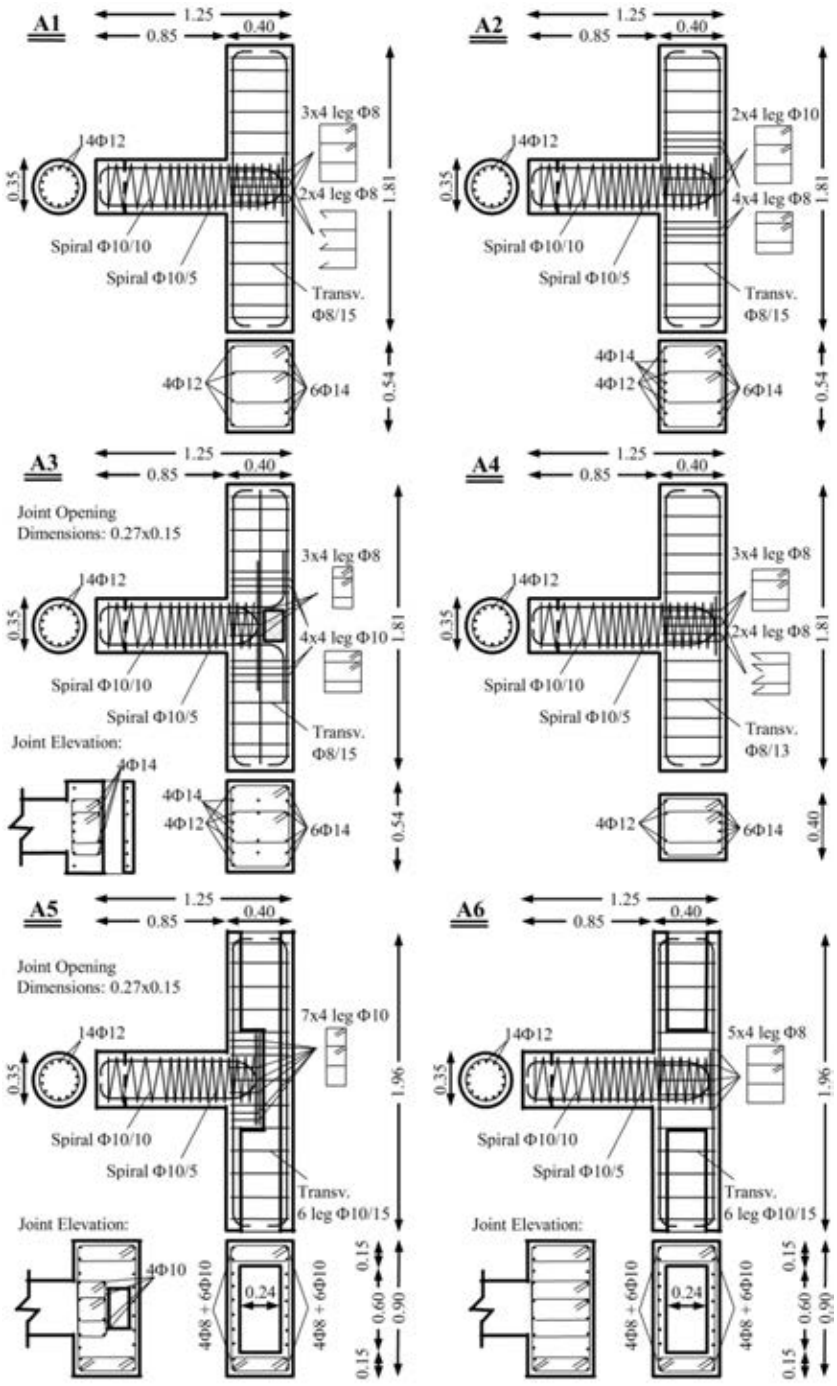

Figure 2: Geometry and reinforcement arrangement for Group A specimens [1].

the empirical expressions for deformation capacity which are included in EN 1998-3, 2005 [7] that completely bypass the requirement of calculating the plastic hinge length. Another approach, initiated by Priestley et al. (1996) [8] and then followed by several other researchers, and the approach to deformability by EN 1998-1, 2004 [9] estimates the plastic hinge length including the length of yield penetration inside the anchorage (see, for example, the detailed analysis in [8]).

In new structural design with EN 1998-1 2004 [9], the plastic hinge length is also used in reinforced concrete (RC) seismic detailing in order to determine the region where additional confinement requirements apply, this is apart from its use in seismic assessment to estimate

the flexural deformation capacity. Due to its importance in these applications as the key to understanding deformability of members, the plastic hinge has been the subject of many experimental and analytical studies and the expressions derived have been quantified and calibrated against several hundreds of tests on isolated column specimens. Still, the disconnect between observation and theory persists, and is considered a major roadblock in establishing the performance criteria for many special categories of members (e.g. walls, columns carrying a high axial load, very slender columns, etc.).

In the typical test, a cantilever column fixed at the base and carrying a constant axial load is driven to a protocol of reversed cyclic lateral load displacement history at the top. Deformation capacity of such members is usually described by the chord rotation that may be sustained by the member prior to loss of its lateral load strength. Apart from the rotation due to flexural curvature that occurs along the length of the member, lumped rotation at the critical section resulting from inelastic strain penetration into the support (e.g. footing) as well as inside the shear span adds up in the reported drift ratios at different levels of performance. This share of deformation is attributed to reinforcement pullout due to the incompatible length change between the bar and the surrounding concrete.

In columns that do not fail by web crushing, pullout rotation increases gradually with imposed drift, claiming a predominant share of the members' deformation capacity near the ultimate limit state.

The following algorithm (Fig. 3) is established in order to define the locations of primary cracks and bar strain, slip and bond distribution along the shear span L_s of a laterally loaded reinforced concrete column as well as the yield penetration length (plastic hinge length). The equations of the proposed algorithm are given in Megalooikonomou et al. 2018 [10]:

Initial Data: Using standard section analysis obtain *M-ϕ (Moment -curvature)* and *M-ε (Moment – Tensile Strain of Reinforcement)* diagrams (or better a unified diagram M-ϕ -ε) given the Axial Load *N* for the typical section of the reinforced concrete column studied:

1st Step: Select value of bar strain, $\varepsilon_o^{(1)}=\varepsilon_o$, after crack formation at the support (Fig. 3).

2nd Step: Find the corresponding moment, M_o at the support, from moment-bar strain diagram. Solve for the length of the disturbed region [10] ℓ_{D1} emanating from the first crack.

3rd Step: Increase strain at critical section to $\varepsilon_o^{(2)} = \varepsilon_o^{(1)} + \Delta\varepsilon_o$. Find the location $x_{cr,2}$ of the second crack. Check if second crack will occur: (a) inside ℓ_{D1}, or (b) in the undisturbed region L_s- ℓ_{D1}.

4th Step: (a) If next crack forms within $\ell_{D1,}$ repeat Step 3 for $\varepsilon_o^{(3)} = \varepsilon_o^{(2)} + \Delta\varepsilon_o$. (b) Otherwise, find the new distrurbed region ℓ_{D2} that extends beyond $x_{cr,2}$.

5th Step: Find total disturbed length, $\ell_{Do}=x_{cr,2}+ \ell_{D2}$

6th Step: Solve for *ε(x) (strain) , s(x) (slip), f_b(x) (bond stress)* for $x_{cr,2}\leq x\leq \ell_{Do}$. In this phase of the solution and up to stabilization of cracking elastic bond is assumed in ℓ_{D2} .

7th Step: Repeat steps 2 to 6 for $\varepsilon_o^{(i)} = \varepsilon_o^{(i-1)} + \Delta\varepsilon_o$ until stabilization of cracking (i.e., no more primary cracks can develop: $\varepsilon_o^{stbl} = \varepsilon_o^{(i)}$). Final length of disturbed zone is obtained from the n^{th} increment using this procedure: $\ell_{Do}=x_{cr,n}+ \ell_{D,n}$.

8th Step: Increase $\varepsilon_o^{(i)} = \varepsilon_o^{(i-1)} + \Delta\varepsilon_o > \varepsilon_o^{stbl}$. Solve for one continuous disturbed region $\ell_{Do} \geq x_{cr,n}+ \ell_{D,n}$ allowing for bond plastification and debonding as well as bar yielding (anchorage solution) up to either (a) ε_o exhausting the ultimate strain of the *M-ε* diagram, or (b) ℓ_{Do} exceeding the available development length of the bar in the shear span, taken here as (L_s+h_{hook}), where h_{hook} refers to the bent length of a hooked anchorage (according with *fib* Model Code (2010) [11] the contribution of a hook to the strength of an anchored bar is $50A_bf_b^{max}$, which corresponds to an additional anchored length, $\Delta L_b=h_{hook}=12.5D_b$). If (b) controls, continue

beyond that point for higher strains using the anchorage solution presented in [10] for the entire length ℓ_{Do}.

9th Step: The last converged value of l_r in the shear span is added to the corresponding yield penetration length into the anchorage resulting in the definition of the total plastic hinge length ℓ_{pl}.

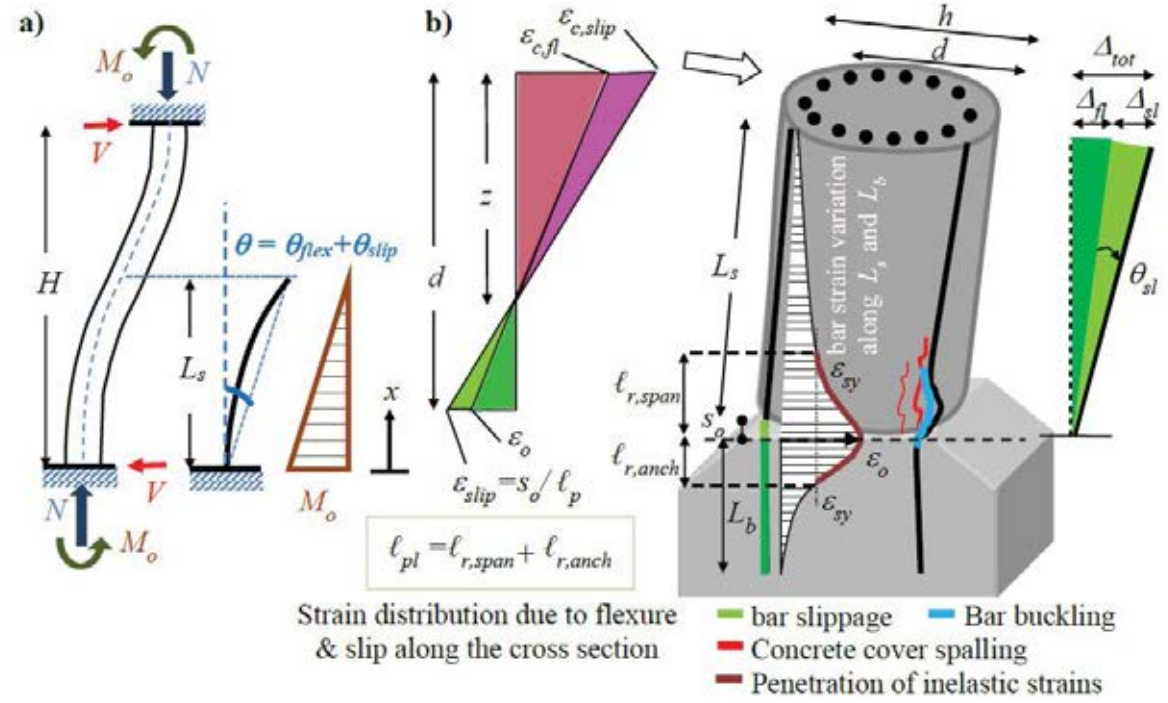

Figure 3: a) Column under lateral sway and b) cantilever model for its deformation analysis

3 CORRELATION WITH THE EXPERIMENTAL RESULTS

It is evident that yield penetration occurs from the critical section towards both the shear span and the support of columns; physically it refers to the extent of the nonlinear region and determines the pull-out slip measured at the critical section. Contrary to the fixed design values adopted by codes of assessment, the yield penetration length is actually the only consistent definition of the notion of the plastic hinge length, whereas the latter determines the contribution of pull-out rotation to column drift and column stiffness. When a reinforced concrete (RC) column is subjected to lateral sway as a result of earthquake action, the large strain demand in the end sections is supported by development of a strain distribution in the anchorage (Fig 3). This causes the bars to displace (or slip) relative to the anchoring concrete at the column fixed end(s). The lumped slip causes rigid-body rotation of the column, thereby alleviating partially the column deformation. This reinforcement slip is assumed to occur in the tension bars only and cause the rotation about the neutral axis. Development of flexural yielding and large rotation ductilities in the plastic hinge zones of frame members is synonymous with the spread of bar reinforcement yielding. Yield penetration in the anchored reinforcing bar inside the shear span of the column where it occurs, destroys interfacial bond between bar and concrete and reduces the strain development capacity of the reinforcement. This affects the plastic rotation of the member by increasing the contribution of bar slippage. Results obtained from the analytical procedures introduced in the previous section are compared here

with experimental evidence from the tests conducted on reinforced concrete bridge piers under cyclic loading reported previously.

In the following figures the aforementioned comparison is depicted and it can be seen that the produced monotonic envelope for applied shear load versus the slip of the extreme tensile reinforcing bar of the circular section of the bridge piers is in good agreement with the experimental evidence [1], [10].

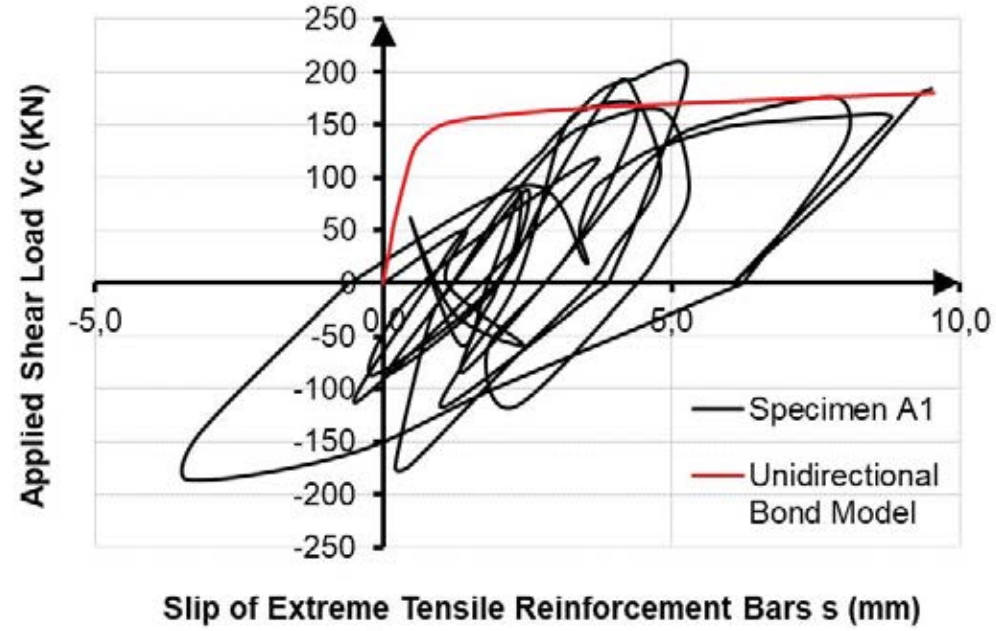

Figure 4: Correlation of the unidirectional bond model with the experimental response of specimen A1.

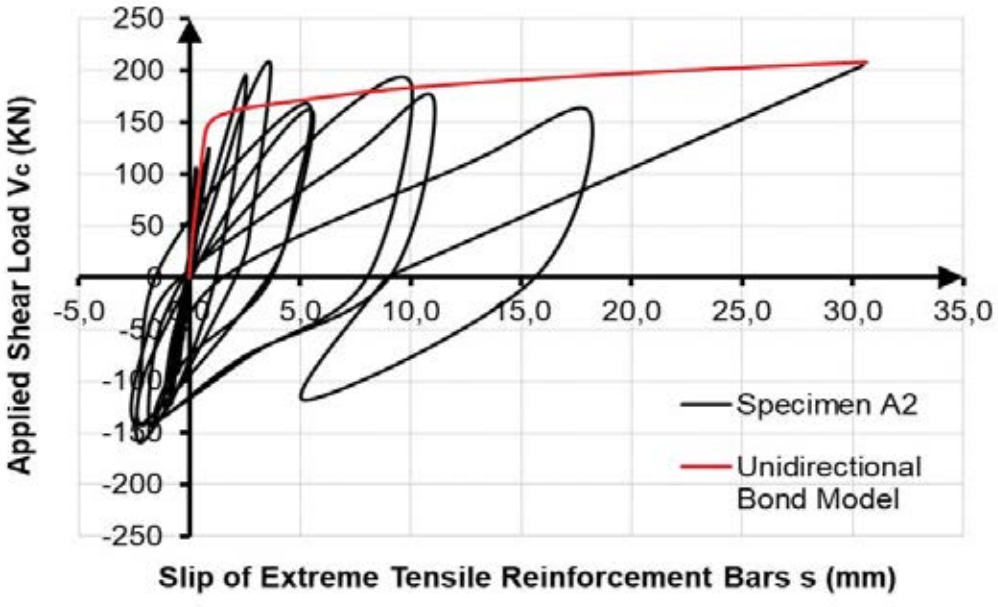

Figure 5: Correlation of the unidirectional bond model with the experimental response of specimen A2.

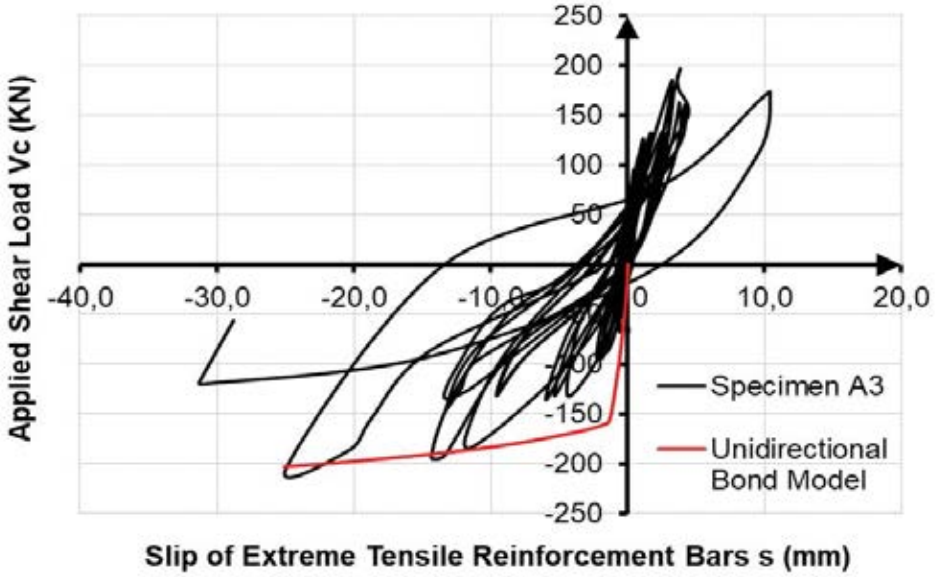

Figure 6: Correlation of the unidirectional bond model with the experimental response of specimen A3.

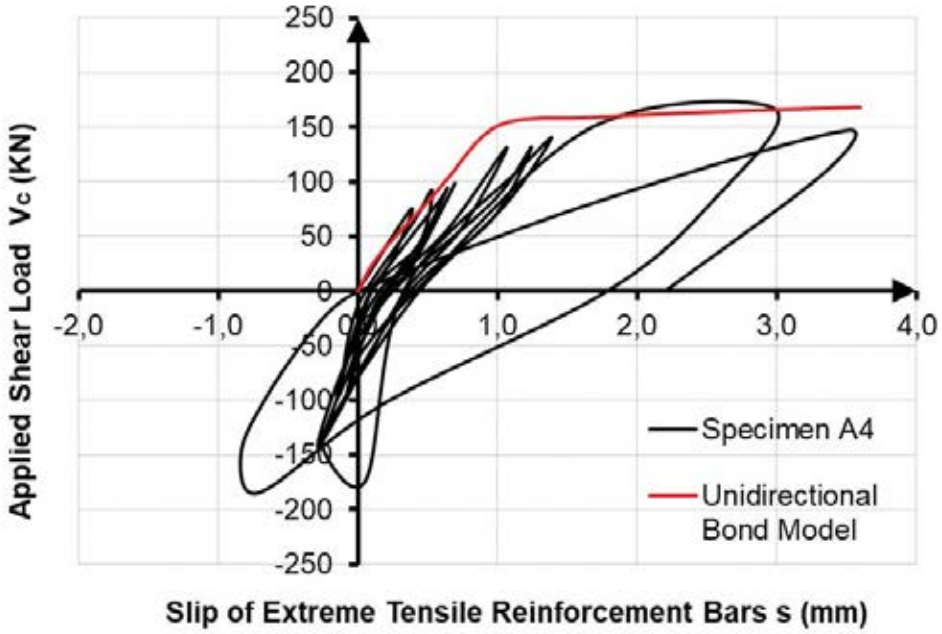

Figure 7: Correlation of the unidirectional bond model with the experimental response of specimen A4.

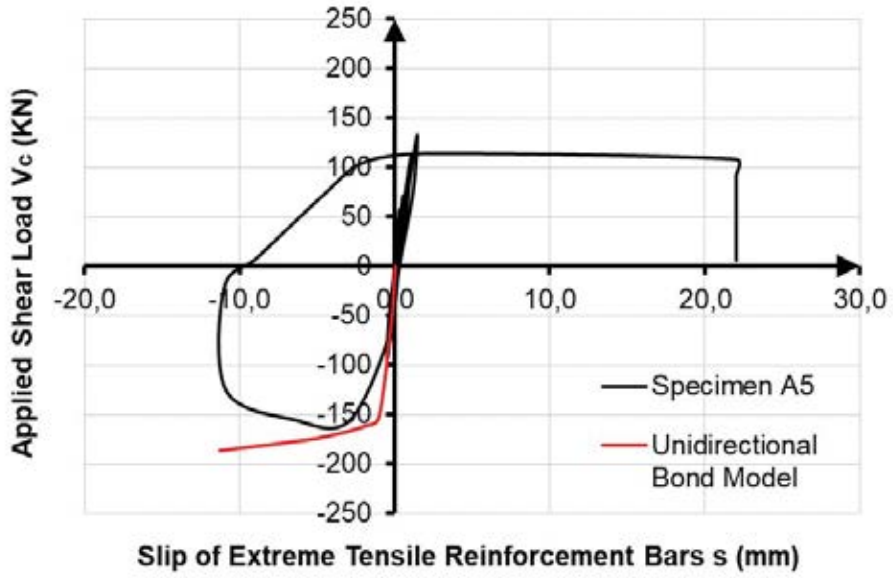

Figure 8: Correlation of the unidirectional bond model with the experimental response of specimen A5.

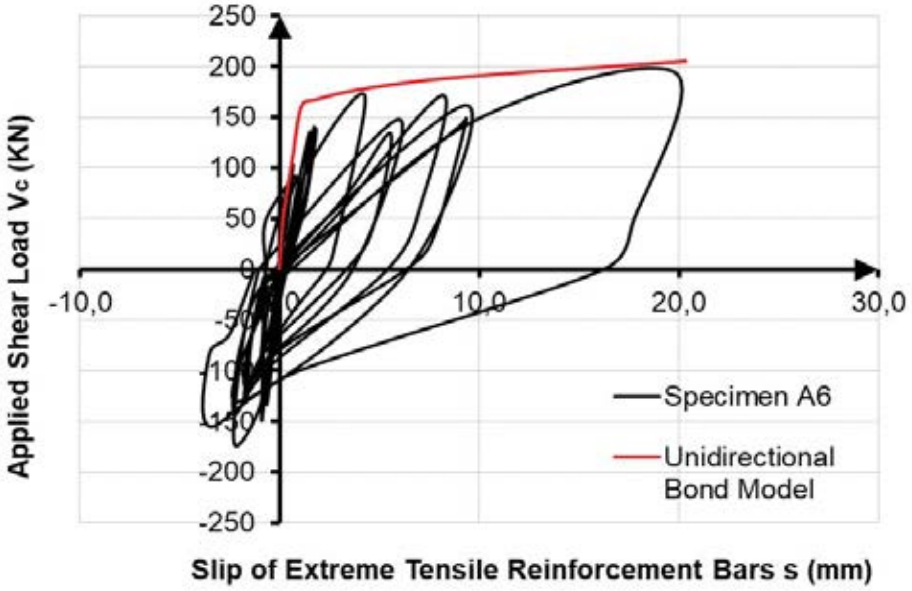

Figure 9: Correlation of the unidirectional bond model with the experimental response of specimen A6.

4 CONCLUSIONS

- The experimental study demonstrated that design and detailing of pier-superstructure monolithic connections according with the EN 1998-2 (2005) [2] leads to a satisfactory performance under earthquake loading. Based on the observed response it was concluded that special care ought to be provided for the design of the anchorages of the pier longitudinal reinforcement according with EN 1992-2 (2005) [4], in order to prevent joint failure due to anchorage pull-out. Placing a fraction of the necessary vertical joint reinforcement in the beams outside the joint, as suggested in EN 1998-2 (2005) [2] for congestion-free alternative detailing did not compromise the strength of the joint, whereas

this practice facilitates placement of the reinforcement during construction. In all cases discontinuities in the joint body such as openings for passage ought to be avoided.

- According to these experimental observations the analytical evidence showed that through the proposed algorithm, the bar strain distributions and the extent of yield penetration from the yielding cross section towards the shear span and towards the support were resolved and calculated analytically by reference to the state of reinforcement strain. The numerical results are well correlated with the experimental evidence and are consistent with the experimental trends described above confirming that the plastic hinge length is controlled by the residual bond that may be mobilized along the yielded reinforcement.

REFERENCES

[1] Timosidis D, Megalooikonomou K.G., Pantazopoulou SJ (2015). Monolithic Reinforced Concrete Bridge Joints under Cyclic Excitation, *Engineering Structures, Vol. 101, p. 477-493*.

[2] EN 1998-2 (2005), Design of Structures for Earthquake Resistance – Part 2 (II): Bridges, CEN, Brussels: European Committee for Standardization.

[3] California Transportation Agency (2004). Caltrans Seismic Design Criteria Ver.3.1.

[4] EN 1992-2 (2005). Design of Concrete Structures – Part 2: Concrete Bridges. Design and detailing rules. European Committee for Standardization, (CEN), Brussels.

[5] Syntzirma D. V., Pantazopoulou S. J. and Aschheim M. (2010). Load history effects on deformation capacity of flexural members limited by bar buckling. *ASCE J. of Structural Eng*.; 136(1): 1−11.

[6] Inel, M., Aschheim, M. and Pantazopoulou, S. (2004). Deformation Indices for Concrete Columns: Predicted vs. Measured. *13thWorld Conf. on Earthquake Engineering*, Vancouver, Canada, No. 2397

[7] EN 1998-3 (2005), Eurocode 8: Design of structures for earthquake resistance -Part 3: Assessment and retrofitting of buildings. European Committee for Standardization (CEN), Brussels.

[8] Priestley, M.J.N., Seible F., and Calvi M. (1996). Seismic Design and Retrofit of Bridges. J. Wiley & Sons Inc., N. York.

[9] EN 1998-1 (2004), Eurocode 8: Design of structures for earthquake resistance – Part 1: General rules seismic actions and rules for buildings, European Committee for Standardization (CEN), Brussels.

[10] Megalooikonomou K.G., Tastani SP, Pantazopoulou SJ. (2018) Effect of Yield Penetration on Column Plastic Hinge Length, *Engineering Structures, Vol. 156, p. 161-174*.

[11] Fib Model Code (2010), Chapter 6: Interface Characteristics, Ernst & Sohn Publications, Berlin, Germany, pp.434.